Available online at www.sciencedirect.com
SCIENCE DIRECT®
Journal of Nuclear Materials 337–339 (2005) 246–250
journal of nuclear materials
www.elsevier.com/locate/jnucmat

Modification of atomic physics rates due to nonlocal electron parallel heat transport in divertor plasmas

F. Allais [a,*], J.P. Matte [a,*], F. Alouani-Bibi [a], C.G. Kim [a], D.P. Stotler [b], T.D. Rognlien [c]

[a] *INRS-Énergie, Matériaux et Télécommunications, 1650 boul. Lionel Boulet, Varennes, Québec, Canada J3X 1S2*
[b] *Princeton Plasma Physics Laboratory, Princeton, NJ, USA*
[c] *Lawrence Livermore National Laboratory, Livermore, CA, USA*

Abstract

The effect of steep temperature gradients on the rate of ionization of atomic hydrogen is studied numerically with the electron kinetic code 'FPI' [Phys. Rev. Lett. 72 (1994) 1208]. A set of cross sections ['Atomic and Plasma-Material Interaction data for fusion'. Supplement to the journal Nucl. Fusion 4 (1993)] has been used which gives the same rates of radiation, ionization and recombination as in the well known edge modeling codes 'UEDGE' and 'DEGAS' for Maxwellian electron energy distribution functions. For this purpose, 30 energy levels are included in the computation, as stepwise ionization is dominant. The enhancement of the ionization rate by non-Maxwellian effects in the colder part of the plasma is significant.

PACS: 52.25.Fi; 52.25.Jm; 52.55.Fa; 52.55.Ff
Keywords: Collisional radiative model; Divertor modelling; Kinetics effects; Parallel transport; UEDGE

1. Introduction

In steep parallel electron temperature gradients, such as those found in the divertors of magnetic fusion devices, the electron heat transport is nonlocal, and the electron velocity distribution function (EVDF) is non-Maxwellian [1–3]. High energy electrons in the tail of the EVDF affect macroscopic properties, such as the rates of ionization and excitation in the cold region. We study in this work some effects of a nonlocal transport on the atomic processes for atomic hydrogen in an advancing heat and ionization front. Our ultimate aim is to develop a nonlocal heat flux model that would allow the hydrodynamic code 'UEDGE' [4] to have not only a correct heat flux along the field lines, as is to be expected from a nonlocal heat flux formula, but also to account for the effects of the non-Maxwellian distributions on the atomic rates. We have used kinetic simulations to establish the nonlocal heat flux formulas and to validate the results in some specific cases [5], and to heat front propagation, (somewhat similar to what will be presented here except that a fully ionized hydrogen plasma was considered) [6].

* Corresponding authors. Tel.: +1 450 929 8127; fax: +1 450 929 8102.
E-mail address: matte@inrs-emt.uquebec.ca (J.P. Matte).

0022-3115/$ - see front matter © 2004 Elsevier B.V. All rights reserved.
doi:10.1016/j.jnucmat.2004.10.089

While there have been several electron kinetic simulations of heat flow along the field lines in divertors [2,3,7] and some did address the enhancement of the ionization rate due to non-Maxwellian effects, these have generally considered only a few excited states. On the contrary, in the 'UEDGE' fluid edge plasma simulation code [4], effective rates for ionization, recombination and radiative energy loss are used, which are tabulated as functions of density and temperature, assuming Maxwellian electron distribution functions, and these, in turn, are based on detailed calculations which include 30 energy levels. These rates are also used in the 'DEGAS2' code [8], and are based on the set of cross-sections by Janev and Smith [9]. This is necessary because ionization from excited states is dominant in the colder part of the plasma. In the present work, (contrary to our previous one [6]) this atomic physics is fully coupled to the free electron distribution function of the electron kinetic code 'FPI' [1,2,10–12], as will be explained in Section 2.

The issue of enhanced ionization due to non-Maxwellian distribution functions is related to non-local electron heat flux, but non-local heat flux formulas do not include this physics. In the present work, we will compare rates obtained by convolutions of the cross sections with the numerically computed electron distribution functions to those obtained with Maxwellians of the same density and average energy (temperature).

2. Ionization model

We consider a hydrogen plasma with both ionized and neutral H atoms. Molecular processes are not taken into account, nor sub-level splitting; only the main quantum number is kept. In Table 1, we list the reactions which are considered for each level or pair of levels, and the symbols for their rates.

The plasma is considered to be optically thin. To compute the rates S_n, α_n, C_{nm}, and β_n, we use the cross sections given in Ref. [9] and $f_0(x, v.t)$ the isotropic component of the velocity distribution function, (written for simplicity $f(v)$). $f(v)$ is either the output of the kinetic Fokker–Planck code 'FPI', or a Maxwellian of the same density and average energy. Rates are then given by:

$$\text{Rate} = N_e\langle\sigma v\rangle = 4\pi\int_{V_{\text{threshold}}}^{\infty} dv v^3\sigma(v)f(v), \tag{1}$$

where $V_{\text{threshold}}$ corresponds to the threshold for the reaction.

The radiative rates A_{mn} are also from [9]. We denote by N_e the density of electrons in the continuum and by N_n the density of neutrals in level n. The time evolution N_n is given by

$$\left(\frac{dN_n}{dt}\right)_{n=1,\infty} = -N_eN_nS_n - N_eN_n\sum_{m\neq n}^{\infty}C_{nm} - N_n\sum_{m=1}^{n-1}A_{nm} + N_e\sum_{m\neq n}^{\infty}N_mC_{mn} + \sum_{m=n+1}^{\infty}N_mA_{mn} + (\beta_n + \alpha_nN_e)N_e^2. \tag{2}$$

Our code directly integrates (2). In a post-processing step, we have also used the collisional radiative *ansatz*, assuming that the time scale for the fundamental level $n = 1$ is very large compared to the time scales of the excited levels. It can be shown that (2) is then equivalent to:

$$\frac{dN_1}{dt} = -S_{\text{eff}}N_1N_e + R_{\text{eff}}N_e^2, \tag{3}$$

where S_{eff} and R_{eff} are the effective ionization and recombination rates. Mass conservation: $N_i + \sum_{n=1}^{30}N_n = N_0$, electro neutrality $N_i = N_e$, and the well known result that most of the neutrals are in the fundamental state $\sum_{n=1}^{30}N_n \approx N_1$ are used to close this system.

We have verified that the rates in [9] are indeed recovered when the EVDF is Maxwellian.

The effect of atomic processes on the free electron distribution function is extremely complicated to compute. Three-body recombination cross sections, angular dependence of cross sections are unknown and it is necessary to introduce simplifications to keep the calculations from being prohibitive. We have assumed that after an inelastic collision, an electron is scattered isotropically and that after an ionizing collision, the secondary electron has negligible energy (it is put in the two first velocity cells), [12].

The atomic physics operator on the electron distribution function may then be written as:

Table 1
List of reactions between each level n ($1 \leqslant n \leqslant 30$) and the continuum and between each pair of levels, n–m ($1 \leqslant n < m \leqslant 30$), and the symbols for their rates

Ionization	$e + H(n) \rightarrow e + e + H^+$	Rate: S_n ($cm^3 s^{-1}$)
Three body recombination	$e + e + H^+ \rightarrow H(n) + e$	Rate: α_n ($cm^6 s^{-1}$)
Excitation and deexcitation	$e + H(n) \rightarrow e + H(m)$	Rate: C_{nm} ($cm^3 s^{-1}$)
Radiative recombination	$e + H^+ \rightarrow H(n) + h\nu$	Rate: β_n ($cm^3 s^{-1}$)
Radiative decay	$H(m) \rightarrow H(n) + h\nu$; $m > n$	Rate: A_{mn} (s^{-1})

$$\left(\frac{\delta f}{\delta t}\right)_{\text{atomic}} = \sum_{n,m}\left(\frac{\delta f_{nm}}{\delta t}\right)^{\text{deexcitation}}_{\text{excitation}} + \sum_{n}\left(\frac{\delta f_n}{\delta t}\right)^{3\text{ body recombination}}_{\text{ionization}} + \sum_{m}\left(\frac{\delta f_m}{\delta t}\right)^{\text{radiative recombination}} \tag{4}$$

and for each level n, we write the ionization-3 body recombination operator as:

$$\begin{aligned}
&\left(\frac{\partial f}{\partial t}\right)_n = \left(\frac{\partial f}{\partial t}\right)_n^{(1)} + \left(\frac{\partial f}{\partial t}\right)_n^{(2)} + \left(\frac{\partial f}{\partial t}\right)_n^{(3)}, \quad \Gamma = m^2\left(\frac{h}{m_e}\right), \quad v_n^2 = \frac{2}{m_e}\frac{13.6\text{ eV}}{n^2};\\
&\left(\frac{\partial f}{\partial t}\right)_n^{(1)} = v\sigma_{\text{ionization}}(v,n)\left[-N_n f(v) + \Gamma F(0) N_e f\left(\sqrt{v^2 - v_n^2}\right)\right] \quad v \geqslant v_n;\\
&\left(\frac{\partial f}{\partial t}\right)_n^{(2)} = \frac{v^2 + v_n^2}{v}\sigma_{\text{ionization}}\left(\sqrt{v^2 + v_n^2}, n\right)\left[-\Gamma F(0) N_e F(v) + N_n f\left(\sqrt{v^2 + v_n^2}\right)\right] \quad v > 0;\\
&\left(\frac{\partial f}{\partial t}\right)_n^{(3)} = \left(N_n N_e S_n - N_e^3 \alpha_n\right)\frac{\delta(v)}{v^2} \quad v = 0.
\end{aligned} \tag{5}$$

For excitation–deexcitation, the operator is similar in form except that the third term is absent, as it corresponds to the addition of secondary electrons by ionization and to the removal of slow electrons by three-body recombination, while the other two correspond to a redistribution of electrons in energy space.

3. First results of the simulation

For the present simulation, we used a 20 m, 1D box with the ions and neutrals treated as cold immobile fluids and with parameters typical of a detached divertor plasma:

$N_0 = N_i + \sum_{n=1}^{30} N_n = 2.5 \times 10^{13}\text{cm}^{-3}$ (uniform). The left and right sides of our simulation box were maintained at constant temperatures of 25 and 1 eV respectively. At $t = 0$, the temperature and ionization were set at 25 eV and 100% between 0 and 2.5 m, and at 1 eV and 10% between 4 and 20 m, with exponential ramps in between. All neutrals were assumed to be in the ground state at $t = 0$. In Fig. 1, we see the temperature profiles at 0 (initial), 2, 5, 25 and 50 μs. The rapid advancement of the heat front is evident. In Fig. 2, we illustrate the free electron density (and hence the degree of ionization) at the same times. It is seen that, at this modest density, there is a time lag between the temperature evolution and the ionization. Compared to a previous simulation with fewer levels, the ionization is more rapid, as expected.

The character of the electron distribution function is quite Maxwellian within 1 m of the left boundary (not shown), because it is near the source (left boundary) temperature of 25 eV. However, within the gradient, at $x = 3.5$ m, as we can see on Fig. 3, the distribution function has changed considerably from the initial single Maxwellian at 2.9 eV. While the bulk has heated up to a temperature of approximately 12 eV, beyond 60 eV,

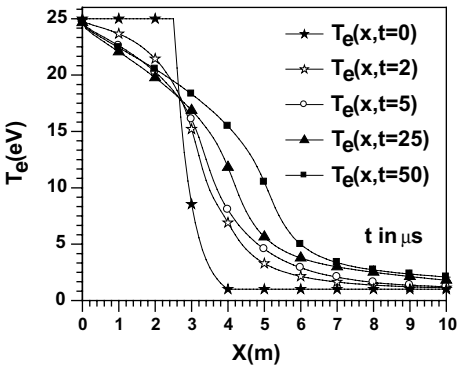

Fig. 1. Time evolution of the temperature profiles as the heat front advances into a 1 eV plasma, while the temperature is maintained at 25 eV at $X = 0$.

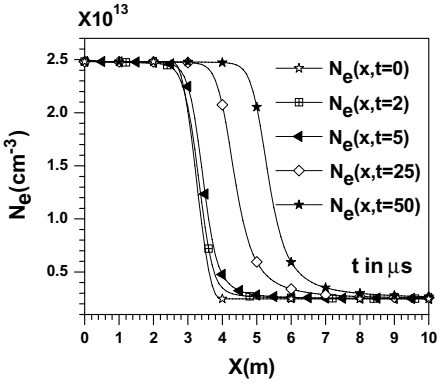

Fig. 2. Time evolution of the free electron density profiles as the ionization front advances. The increase is entirely due to ionization.

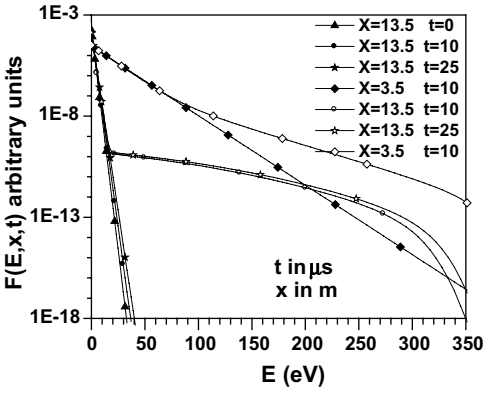

Fig. 3. (Black dots): Electron energy distribution functions. (Void dots): Maxwellians at the same densities and average energies for $x = 13.5$ m, at $t = 0$, 10 and 25 μs, and at $x = 3.5$ m at 10 μs.

there is a hot tail at the hot side's temperature of 25 eV. Deep in the cold plasma, at $x = 13.5$ m, the bulk has hardly heated up compared to its original 1 eV temperature, but there is now an important hot tail, which begins near 20 eV, and it changes very little after a few microseconds.

The effect of these distribution functions on the effective ionization rate is illustrated in Fig. 4. It is strongly enhanced beyond $x = 5$ m. but not at $x = 3.5$ m because the distribution there (Fig. 3) is fairly Maxwellian up to 60 eV, and it is these bulk electrons which do most of the excitation and ionization. On the contrary, at $x = 13.5$ m, the hot tail's participation (see Fig. 3) to ionization and excitation is dominant, hence an orders of magnitude enhancement of S_{eff} there. The recombination rate is modified somewhat, but much less, by this deformation of the electron distribution function.

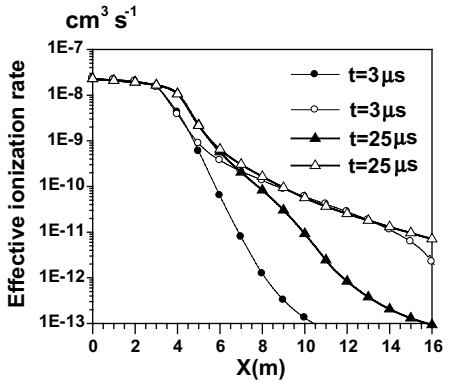

Fig. 4. Effective ionization rates obtained from the ≪FPI≫ electron velocity distributions (open dots) and from Maxwellians distributions (closed dots) at the same density and average energy, for $t = 3$ and 25 μs.

4. Conclusion

Our electron kinetic code 'FPI' has been upgraded to include the ionization of atomic hydrogen (or its isotopes), with 30 energy levels, so that the rates of ionization are compatible with those used by the well known codes 'UEDGE' and 'DEGAS', when the electron distribution function is Maxwellian. It was shown that in a steep temperature gradient, the global ionization rate is greatly enhanced in the colder part of the plasma, due to the presence of a hotter component which results from nonlocal heat transport. It remains to improve the code to include the effects of hydrodynamic motion and recycling from the plate and of heating due to cross-field transport as in [3] (instead of a fixed hot temperature at the left end) and to develop an effective nonlocal formula for correcting the effective ionization rate in the presence of steep temperature gradients in 'UEDGE', analogous to our nonlocal heat flux formula [5]. The inclusion of hydrogen molecular effects and of impurities is also left for future work.

Acknowledgments

The INRS authors thank the department of Science and Technology of Quebec and the National Research Council of Canada for their support. D.P.S. and T.D.R. are supported by the Office of Fusion Energy of the US Department of Energy.

References

[1] J.P. Matte, J. Virmont, Phys. Rev. Lett. 49 (1982) 1936.
[2] Z. Abou-Assaleh, R. Marchand, J.P. Matte, et al., Contrib. Plasma Phys. 30 (1990) 37;
Z. Abou-Assaleh, J.P. Matte, et al., Contrib. Plasma Phys. 32 (1992) 268;
Z. Abou-Assaleh, M. Petravic, et al., Contrib. Plasma Phys. 34 (1994) 175.
[3] O. Batishchev et al., J. Nucl. Mater. 241–243 (1997) 374;
Phys. Plasmas 4 (1997) 1672;
J. Plasma Phys. 61 (1999) 347.
[4] T.D. Rognlien et al., J. Nucl. Mater. 241–243 (1997) 590;
T.D. Rognlien et al., Phys. Plasmas 6 (1999) 1851.
[5] F. Alouani Bibi, J.P. Matte, Phys. Rev. E 66 (2002) 066414;
F. Alouani Bibi and J.P. Matte, Proceedings of the 29th European Physical Society Conference on Plasma Physics and Controlled Fusion, Montreux, Switzerland, 17–21 June 2002. Paper P5.013.
[6] F. Allais, J.P. Matte, F. Alouani-Bibi, D. Stotler, in: Proceedings of the 29th European Physical Society Conference on Plasma Physics and Controlled Fusion, Montreux, Switzerland, 17–21 June 2002. Paper P3.215.

[7] K. Kupfer et al., Phys. Plasmas 3 (1996) 3644.
[8] D.P. Stotler, C.F.F. Karney, Contrib. Plasma Phys. 34 (1994) 392.
[9] R.K. Janev, J.J. Smith, Atomic and plasma-material interaction data for fusion, Supplement to the Journal Nuclear Fusion 4 (1993); ALADDIN data base (http://www-amdis.iaea.org/aladdin.html).
[10] J.M. Liu et al., Phys. Rev. Lett. 72 (1994) 2717; Phys. Plasmas 1 (1994) 3570.
[11] J.P. Matte et al., Phys. Rev. Lett. 72 (1994) 1208.
[12] S. Ethier, J.P. Matte, Phys. Plasmas 8 (2001) 1650.